Theoretical Study of the Reactivity of Fe^+ toward OCS

Dongju Zhang, Chengbu Liu,* and Wensheng Bian

College of Chemistry and Chemical Engineering, Shandong University, Jinan, 250100, People's Republic of China

Received: April 16, 2003; In Final Form: July 29, 2003

The reactivity of Fe^+ toward OCS on both quartet and sextet potential energy surfaces have been investigated at the B3LYP/6-311+G(d) level of theory. Various intermediates, transition states, and products involved in the reaction of Fe^+ with OCS are presented, and the details of the mechanisms of C−S and C−O bond activations are revealed. The calculated results indicate both the C−O and C−S bond activations proceed according to an insertion−elimination mechanism, which could be general for the reactions of first-row transitions with small sulfide molecules. The C−S bond activation is found to be much more favorable than the C−O bond activation. The energetically most favorable reaction is $Fe^+(^6D) + OCS \rightarrow FeS^+(^6\Sigma_g) + CO$, endothermic by 1.8 kcal mol^{-1}. The ground states of products $FeCO^+$ and $FeCS^+$, which cannot be specified by early experiments, have been confirmed to be in their quartets. All theoretical results are in good agreement with early experimental observations.

1. Introduction

The chemistry of transition metal sulfur systems has attracted increasing attention due to their industrial and biological relevance.[1] The industrial interest of transition metal sulfur species includes catalysis,[2] corrosion,[3] lubrication,[3] battery technology,[4,5] etc. In many biological systems, it has been found that sulfur coordination is necessary for the functioning of numerous biological transition metal centers as a key part of its active site.[6,7] Nowadays, many transition metal sulfides have been utilized as enzymes and heterogeneous catalysts, where transition metal centers play an important role as potentially reactive sites and are capable of reacting with a large number of small molecules such as H_2, C_2H_6, H_2O, O_2, SO_2, and OCS. Recently, the reactions of M^+ (M = Fe and Co) with the sulfur-transfer reagent CS_2 and OCS have been inspected experimentally using guided ion beam mass spectrometer (GIB) by the Armentrout group,[8] where metal-sulfide bond energies were determined and relevant mechanism were proposed. In these reactions, MS^+ is found to be dominant product at the low-energy condition. From the determined thermochemistry data, they predicted the formation of MS^+ species proceeds via an insertion−elimination mechanism. In a more recent paper,[9] we reported the theoretical study of the reaction of Fe^+ with CS_2, in which all experimentally observed results had been rationalized. The reaction of M^+ with OCS may be more complicated than its reaction with CS_2, because there are both C−O and C−S bonds in OCS whereas only the C−S bond exists in the CS_2 molecule. The C−S bond energy (3.14 eV)[10] in OCS is lower than in CS_2 (4.50 eV),[10,11] so MS^+ species can be expected to form easily from the reaction of M^+ with OCS. On the other hand, the C−S bond energy in OCS is 3.74 eV lower than the C−O bond energy (6.88 eV),[11] suggesting that the C−S bond is much weaker than the C−O bond. In other words, reaction 1 could not compete with reaction 2 at the low-energy condition.

$$M^+ + OCS \rightarrow MO^+ + CS \quad (1)$$

$$M^+ + OCS \rightarrow MS^+ + CO \quad (2)$$

From the measured thresholds in the $Fe^+ + CS_2$ system, Rue and Armentrout proposed that for the $Fe^+ + OCS$ system, reaction 2 was endothermic by 1.8 kcal mol^{-1}, an approximately thermoneutral process, whereas reaction 1 was endothermic by 78.6 kcal mol^{-1}.[8] Although the experimental study has provided accurate thermochemical data for the $M^+ + OCS$ (M = Fe, Co) system, the detailed information of the potential energy surface of $[M, C, O, S]^+$ is still scarce, and further, confirmation of the relevant mechanism needs the assistance of theory. As a supplement of the experimental study, we present here a theoretical study of the reactivity of Fe^+ toward OCS. Calculated results are expected to calibrate experimental findings and to give new suggestions that could not be reached experimentally under the considered conditions.

The present reaction involves an open-shell transition metal system, where the electron correlation effect is expected to play an important role in determining system energetics and electronic configurations. It is known that the accurate theoretical treatment of open-shell transition metal systems is still difficult with conventional ab initio molecular orbital theory, because a relatively large number of electrons is present in these systems. As an alternative, density functional theory[12,13] (DFT) and, in particular, DFT/HF hybrid methods have been widely applied to electronic structure calculations on systems containing transition metals. These methods combine reasonable computational costs with accuracy sufficient for describing open-shell transition metal systems.

2. Computational Methods

In the present work, the B3LYP functional[14,15] is chosen, which includes three fitted parameters and a mixture of Hartree−Fock exchange and DFT exchange corrections. This choice is motivated by its successful performance for many open-shell transition metal compounds.[16,17] Previous investigations[18−20] have underlined the reliability of the B3LYP functional for

* Corresponding author. E-mail: cbliu@sdu.edu.cn.

10.1021/jp035018l CCC: $25.00
Published on Web 09/30/2003

TABLE 1: Theoretical and Experimental Bond Dissociation Energies at 0 K (eV)

species	calc	exp	species	calc[a]	exp
SC−O	6.93	6.88 ± 0.04[b]	Fe^+−O	3.49	3.47 ± 0.06[e]
OC−S	3.10	3.140 ± 0.005[b]	Fe^+−S	3.14	3.08 ± 0.04[f]
SC−S	4.58	4.50 ± 0.04[b,c]	Fe^+−CO	1.81	1.36 ± 0.08[g]
CS	6.97	7.37 ± 0.04[c]	Fe^+−CS	2.91	2.40 ± 0.12[f]
CO	10.80	11.109 ± 0.005[d]			

[a] With respect to Fe^+ (^{6}D). [b] Reference 10. [c] Reference 11. [d] Reference 27. [e] Reference 28. [f] Reference 29. [g] Reference 30.

describing potential energy surfaces (PES), predicting electronic structures, calculating thermochemical properties for systems containing transition metal. For coordinatively unsaturated iron compounds, the calculated average error of the relative energies with B3LYP has been estimated to be within ±0.3 eV.[21] For the present calculations, this functional was combined with the standard 6-311+G(d) basis set.[22,23] This basis set is flexible enough to give a good account of longer range ion−ligand interactions and is also large enough to generally reduce the basis set superposition error to less than the errors inherent in the method, so that superposition error corrections become unnecessary. The choice of the B3LYP/6-311+G(d) level of theory is also promoted by its successful performance for the reaction of FeS^+ with CH_4 reported early by Barsch et al.,[24] where reasonably accurate information of the potential energy surface of [Fe, S, C, H_4]$^+$ has been unraveled.

The geometries and energies of various species involved in the reaction of Fe^+ toward OCS were first obtained at the chosen level of theory. All structures discussed in the text correspond to fully optimized geometries with both the gradients and the displacements from analytical second derivatives below the standard convergence criteria. Spin contamination of the unrestricted B3LYP open-shell determinants was in all cases small, and the deviation of the S^2 expectation values for the open-shell species involved here never exceeded 5%. Vibration analyses were performed for all optimized stationary points to determine their characters (minimum or first-order saddle point) and to evaluate the zero-point vibrational energies (ZPE), which were included in all relative energies to allow for a direct comparison to experiment. The pathways between the transition structures and their corresponding minima have been identified by intrinsic reaction coordinate (IRC) calculations.[25] All calculations were performed with the Gaussian 98 program package[26] on the SGI Origin 2000 Server.

3. Results and Discussion

In the following sections, we will first establish accuracy that can be expected from the chosen B3LYP/6-311+G(d) level of theory for the Fe^+ + OCS system. Then, we will present the theoretical results for various intermediates, transition states (TS), and products involved in the reaction of Fe^+ with OCS and discuss the mechanisms of C−S and C−O bond activations in light of the recent experimental and theoretical data available. Finally, the present results will be compared with our earlier conclusions drawn from Fe^+ + CS_2 system.

3.1. Evaluation of the Computational Accuracy. To evaluate the reliability of the chosen level of theory, we calculated the bond dissociation energies (BDE) for several species involved in the reaction of Fe^+ with OCS, and the relevant results were shown in Table 1, where the available experimental values were also listed for comparison. As shown in Table 1, most of the theoretical values are in good agreement with experimental findings. Although the errors of the BDEs for Fe^+−CO and Fe^+−CS species are larger than for the others, the tendency is accordant with that of the experimental values. According to these BDEs, the relative stabilities of two main exit channels expressed by reactions 1 and 2 to the entrance channel are estimated to be endothermic by 79.3 and 0.9 kcal mol^{-1}, respectively, and reproduce the experimentally determined values, 78.6 and 1.8 kcal mol^{-1}. From these relative energies, we are confident in the ability of the chosen level of theory to describe the features of the PES of [Fe, C, O, S]$^+$.

TABLE 2: Theoretical and Experimental Properties for the Ground State OCS Molecule[a]

	R_{C-S}	R_{C-O}	ω_1	ω_2	ω_3
calc	1.568	1.157	2115	876	512 (2)
exp[b]	1.561	1.156	2072	866	520 (2)

[a] The symbols R and ω denote the bond length (Å) and vibrational frequencies (cm^{-1}), respectively. [b] Reference 31.

3.2. Reactants and Products. For the OCS molecule, one of the reactants, we calculated its properties, including the geometry, vibrational frequencies, and C−O and C−S bond dissociation energies. The relevant results are shown in Tables1 and 2, respectively. Clearly, the B3LYP functional reproduces all properties of the OCS molecule well. However, for another reactant, Fe^+, B3LYP theory cannot predict its asymptotic difference between the ground state (^{6}D, 3d^{6}4s^1) and first excited state (^{4}F, 3d^7) correctly. Experimentally, the ground state of Fe^+ is determined to be 5.8 kcal mol^{-1} more stable than its first excited state.[32] However, at the employed level of theory, the ^{4}F atomic state is calculated to be 4.9 kcal mol^{-1} more favorable than the ^{6}D atomic state. This error is in general attributed to the deficiency of the one-particle basis set and the defect of DFT in describing atomic asymptotes, which makes rather a favorite of the d^n configurations over d^{n-1}s^1.[33] In the present work, however, our main goals are to examine the detailed reaction mechanism, and to evaluate the relative energies of the species involved in the reaction of Fe^+ toward OCS rather than to calculate their accurate absolute values. Thus we did not simply correct the calculated error for the atomic states of Fe^+, and only made a comparison of the relative energies of the various species involved here. All the relative energy given below refer to the Fe^+ (^{6}D) + OCS, and that of the corresponding reactant on the quartet surface, Fe^+ (^{4}F) + OCS, is taken as 5.8 kcal mol^{-1} by using the experimental excitation energy (0.25 eV, or 5.8 kcal mol^{-1}) from Fe^+(^{4}F) to Fe^+ (^{6}D).

Because the separation between the two atomic states, Fe^+-(^{4}F) and Fe^+(^{6}D), is only 5.8 kcal mol^{-1}, the sextet and quartet surfaces of [Fe, C, O, S]$^+$ could be so close that the intersystem crossing between two surfaces would occur in course of the reaction of Fe^+ with OCS. Thus the present calculations were performed on both quartet and sextet surfaces of [Fe, C, O, S]$^+$. Our calculations include two conceivable reaction mechanisms that differ by the initial orientation of Fe^+ relative to the C−O or C−S bond being activated. Early experimental observations[8] indicated FeS^+ and $FeCO^+$ are main products at low energies, and FeO^+ is also monitored at higher energies. According to these clues, we optimized the structures of various possible products, as shown in Figure 1. Our calculations predict a $^6\Sigma^+$ ground state for both FeS^+ and FeO^+, and are in agreement with recent literature.[24,34,35] The energetically lowest quartets for FeS^+ and FeO^+ are calculated to be 5.47 and 8.52 kcal mol^{-1} above the corresponding ground state, respectively. For $FeCO^+$ and $FeCS^+$, their ground states are found to be in ^{4}A″ states, and the corresponding sextet states are calculated to 26.0 and 22.1 kcal mol^{-1} less stable, respectively. Form Figure 1, it is clear that the geometrical structures of $FeCO^+$ and $FeCS^+$

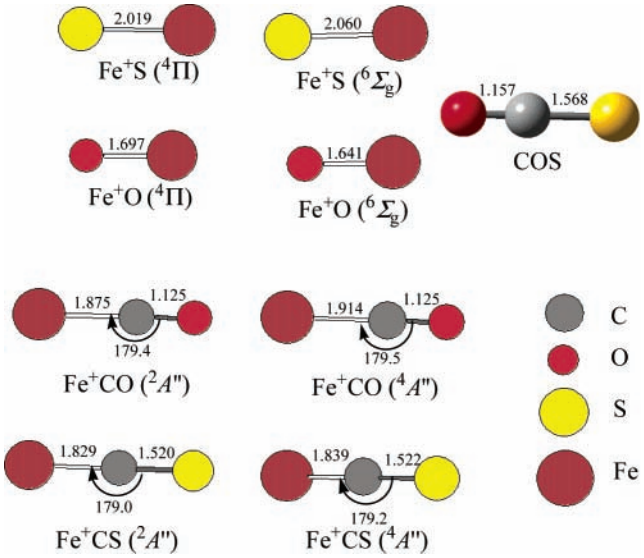

Figure 1. Optimized geometrical parameters for the reactant and products on both quartet and sextet PESs of $[Fe, C, O, S]^+$ at the B3LYP/6-311+G(d) level of theory (distances in ångstroms and angles in degrees).

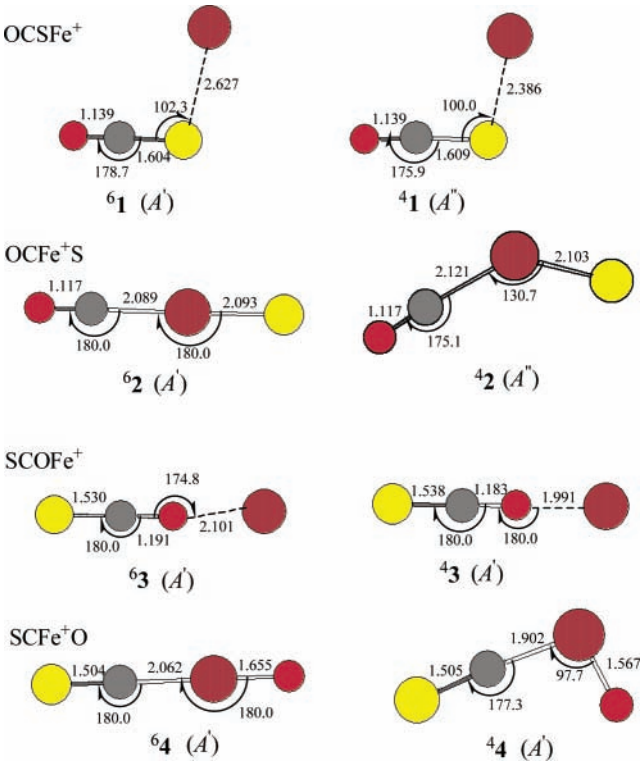

Figure 2. Optimized geometrical parameters for the intermediates on both quartet and sextet PESs of $[Fe, C, O, S]^+$ at the B3LYP/6-311+G-(d) level of theory (Distances in ångstroms and angles in degrees).

including their quartet and doublet species are almost linear. Our calculations started from C_s structures, and the optimizations led them to $C_{\infty v}$ symmetry.

3.3. Encounter Complexes. As Fe^+ and OCS approach each other, there are two possible encounter complexes: sulfur-bound structures ^{6}**1** and ^{4}**1**, and oxygen-bound structures ^{6}**3** and ^{4}**3**. Their geometrical parameters are collected shown in Figure 2 again, where the superscripts denote the spin multiplicities. All four complexes are found to have C_s symmetry. For the sulfur-bound structures, the calculations predict a ^{4}A″ quartet ground state (^{4}**1**) at relative energy to separate reactants $E_{rel} = -28.4$ kcal mol^{-1}, whereas the sextet analogue (^{6}**1**) is in the ^{6}A′ state

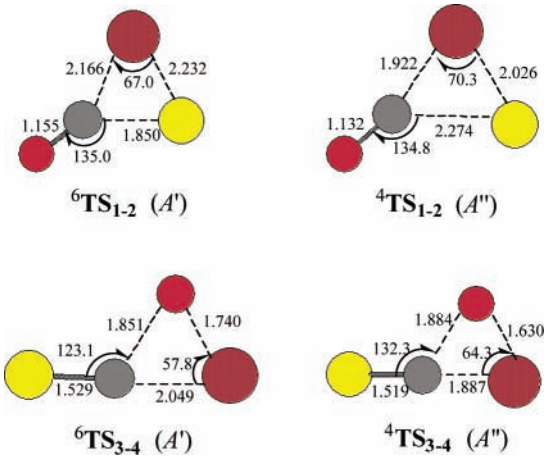

Figure 3. Optimized geometrical parameters for the saddle points on both quartet and sextet PESs of $[Fe, C, O, S]^+$ at the B3LYP/6-311+G-(d) level of theory (distances in ångstroms and angles in degrees).

and its energy is calculated to be 12.8 kcal mol^{-1} less stable than ^{4}**1**. In ^{6}**1**, the OCS moiety is bound to iron at a distance $r_{Fe-S} = 2.627$ Å with an FeSC angle of 102.3°, whereas in ^{4}**1** the Fe−S distance and FeSC angle are 2.386 Å and 100.0°, respectively, smaller than those in ^{6}**1**, indicating the interaction between two reactants is stronger. For oxygen-bound encounter complexes, its ground state is found to be also in its quartet (^{4}**3**, ^{4}A″) at $E_{rel} = -25.6$ kcal mol^{-1}; however, the corresponding ^{6}A′ sextet complex (^{6}**3**) is very close in energy ($E_{rel} = -22.8$ kcal mol^{-1}). These results indicate that the intersystem crossing between the quartet and sextet surfaces seems possible as Fe^+ approaches either the sulfur or oxygen atom in OCS to lead the system to the most energetically favorable pathway. As seen in Figure 2, ^{6}**3** shows a quasi-linear geometry at a distance $r_{FeO} = 2.101$ Å with an Fe−O−C angle of 174.8°, whereas ^{6}**3** has a linear structure at slightly smaller Fe−O distance (1.991 Å). Compared to the geometrical parameters of free OCS molecule (see Figure 1), we found that OCS unit in these four encounter complexes are only distorted slightly, indicating a weakly electrostatic interaction in nature between Fe^+ and OCS in these complexes.

From these encounter complexes, the C−S and C−O bonds would be activated along the reaction pathways to form various products. In the following sections, we will discuss the interactions of the iron cation with the C−S and C−O bonds one by one.

3.4. C−S Bond Activation. Starting from the sulfur-bound encounter complex, two C−S bond activation mechanisms can be expected: one is Fe^+ inserts into the C−S bond to form the OC−Fe^+−S intermediate, whose dissociation results in the formation of FeS^+, and the other is Fe^+ directly abstracts the sulfur atom from OCS. The geometries of inserted intermediates (^{6}**2**, ^{4}**2**) of the C−S bond on the quartet and sextet surfaces are shown in Figure 2. ^{6}**2** has a linear structure ($C_{\infty v}$ symmetry) and is the ground state of the inserted intermediates with a energy of 27.2 kcal mol^{-1} below the entrance channel. ^{4}**2** has C_s symmetry with a S−Fe−C angle of 130.7°, and its energy is calculated to be 7.2 kcal mol^{-1} less stable than ^{6}**2**. The encounter complex **1** and the inserted structure **2** are connected by $\mathbf{TS_{1-2}}$ (see Figure 3), which have been confirmed by IRC calculations. The sextet and quartet TSs ($^6\mathbf{TS_{1-2}}$ and $^4\mathbf{TS_{1-2}}$) are localized at $E_{rel} = +6.9$ and -12.6 kcal mol^{-1}, respectively. Structurally, the two TSs are similar, having three-membered-ring structures with C_s symmetry. The imaginary frequency is 225i cm^{-1} for $^6\mathbf{TS_{1-2}}$, and 199i for $^4\mathbf{TS_{1-2}}$, and the correspond-

ing normal modes correspond to the rupture of C−S bond and the formations of Fe−C and Fe−S bonds. In ^{4}**TS$_{1-2}$**, the breaking C−S is notably longer than in ^{6}**TS$_{1-2}$** (1.850 Å for the former, and 2.274 Å for the latter), suggesting that the quartet TS could be a late saddle point on its PES. The exit channels along the C−S bond activation branch are the direct dissociation of the insertion intermediate **2**. There are two possible pathways: Fe−S and Fe−C bond ruptures, resulting in the products $FeCO^+ + S$ and $FeS^+ + CO$, respectively. Calculated results indicate that Fe−C bond rupture of ^{6}**2** is the generically most favorable exit channel, the overall reaction $Fe^+(^6D) + OCS \rightarrow FeS^+ (^6\Sigma_g) + CO$ is calculated to be endothermic by 0.9 kcal mol^{-1}. This is in good agreement with the experimental determination (1.8 kcal mol^{-1}).[8] The Fe−C bond rupture of ^{4}**2** is a slightly less favorable channel from the view of energy, and the overall reaction $Fe^+(^4F) + OCS \rightarrow FeS^+ (^4\Pi) + CO$ is endothermic by 5.5 kcal mol^{-1}. The Fe−S bond ruptures of intermediate ^{6}**2** and ^{4}**2** to form $FeCO^+$ and S are much more difficult, and the overall reactions $Fe^+(^6D) + OCS \rightarrow FeCO^+ (^4A'') + S(^3P)$ and $Fe^+(^4F) + OCS \rightarrow FeCO^+(^2A'') + O(^3P)$ are calculated to be endothermic by 29.7 and 52.9 kcal mol^{-1}, respectively. The high-energy requirements indicate these two processes are energetically less favorable at low energies. The energy profile along the C−S bond activation branch for the reaction of Fe^+ with OCS is summarized in Figure 4a. It is seen that the PES crossing between quartet and sextet surfaces occurs twice along the C−S bond activation branch: in the course of the approach of Fe^+ and OCS each other and in the course of the conversion of **TS$_{1-2}$** to **2**.

From the discussion above, it is clear it the C−S bond activation involves an insertion−elimination mechanism. In addition, as mentioned above, it could be possible that direct S atom abstraction from OCS also contributes to the formation of FeS^+. To show the relevant mechanism, a transition structure of the type $[Fe---S---C-O]^+$ was designed; however, the structure always collapsed to the encounter complex **1** on both quartet and sextet surfaces during the geometry optimizing, indicating that there is no tight transition state for the direct abstraction reaction.

3.5 C−O Bond Activation. We now turn to the second part of the PES of $[Fe, C, O, S]^+$, the C−O bond activation branch. The intermediates and transition states involved along this branch are again collected in Figures 2 and 3, and the resulting energy profile is shown in Figure 4b. Similar to the C−S bond activation, the involved mechanism for the C−O activation is also found to be an insertion−elimination process, and the present calculations give no evidence of the direct oxygen atom abstraction by Fe^+ from OCS. This activation branch starts from the oxygen-bound encounter complex, **3**. According to the insertion−elimination mechanism, the next steps on both sextet and quartet surfaces are considered as Fe^+ inserting into the C−O bond, to form intermediates ^{6}**4** and ^{4}**4**, respectively. The geometries of the C−O bond inserted intermediates are similar to those corresponding C−S inserted intermediates discussed above. ^{6}**4** has a linear structure with a $C_{\infty v}$ symmetry, and ^{4}**4** has C_s symmetry with a O−Fe−C angle of 97.7°. The energies of ^{6}**4** and ^{4}**4** are calculated to be 22.6 and 25.0 kcal mol^{-1} above the separate reactants, respectively, much higher than those of ^{6}**2** and ^{4}**2** (cf. Figure 4a,b). The initial complex **3** and the inserted intermediate **4** are connected by **TS$_{3-4}$**, a first-order saddle point of C−O bond activation. The energies of the sextet and quartet TSs, ^{6}**TS$_{3-4}$** and ^{4}**TS$_{3-4}$**, are located at 53.4 and 33.7 kcal mol^{-1} above the reactants, and the corresponding to imaginary frequencies are 579i and 460i, respectively. Comparing Figure

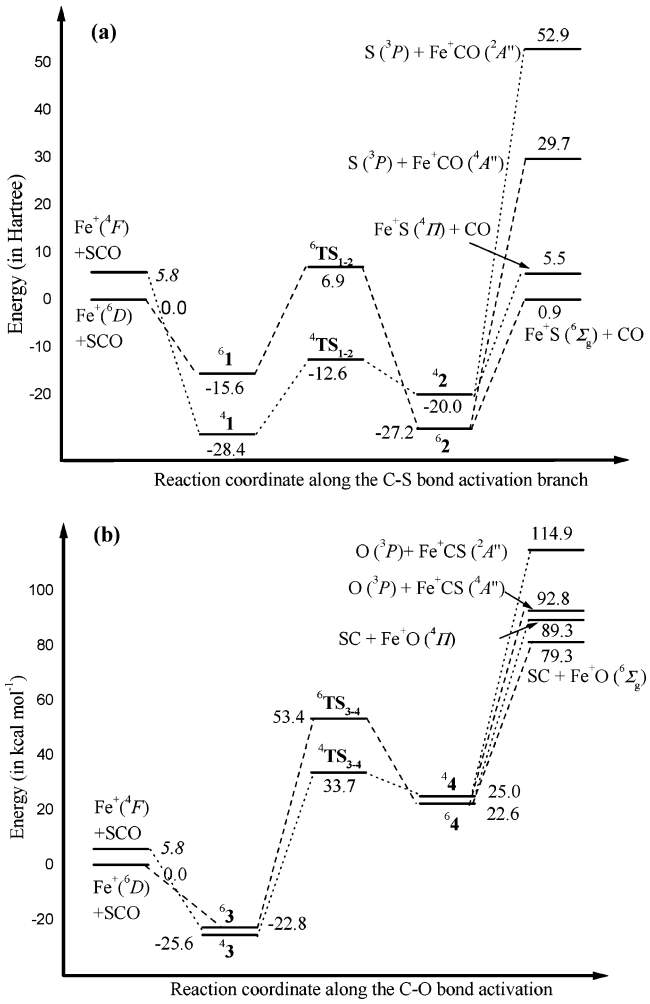

Figure 4. Potential energy surface profiles (a) along the C−S bond activation branch and (b) along the C−O bond activation branch. The dotted lines denote the quartet surface, and the dashed lines denote corresponding sextet surface. The relative energy of $Fe^+(^4F) + OCS$ is obtained from the experimental splitting between the ^{6}D and ^{4}F atomic states of Fe^+ and is given in italics.

4a with Figure 4b, we noted that the energy barriers for C−O bond activation on both quartet and sextet PESs are much higher than those corresponding C−S bond activation, suggesting the C−O bond activation is much less favorable than the C−S bond activation and only feasible at elevated energies. Similar to intermediate **3**, there are two possible dissociation channels from intermediate **4**: the Fe−C bond rupture to form FeO^+ and CS, and the Fe−O bond rupture to form $FeCS^+$ and an O atom. Our calculations show that the Fe−C bond rupture is more favorable than the Fe−O bond rupture. From Figure 4b, it is clear that the reaction $Fe^+(^6D) + OCS \rightarrow FeO (^6\Sigma_g) + SC$ is the energetically more favorable channel at elevated energies, which is endothermic by 79.3 kcal mol^{-1} and in good agreement with the experimental determination, 78.6 kcal mol^{-1}, whereas the reaction on the quartet surface reaction $Fe^+(^4F) + OCS \rightarrow FeO (^4\Pi) + SC$ is 10.0 kcal mol^{-1} more endothermic than that on the sextet surface. Two reactions corresponding to the Fe−O bond rupture to form $FeCS^+$ are calculated to be highly endothermic by 92.8 and 114.9 kcal mol^{-1}, respectively. Thus it is quite reasonable that the $FeCS^+$ species was not experimentally monitored in the $Fe^+ + OCS$ system. From Figure 4b, we found that the PES crossing behavior along the C−O bond activation branch is also similar to the C−S bond activation branch: the sextet surface may cross into the quartet surface as ground-state Fe^+ and OCS approach each other, and the system

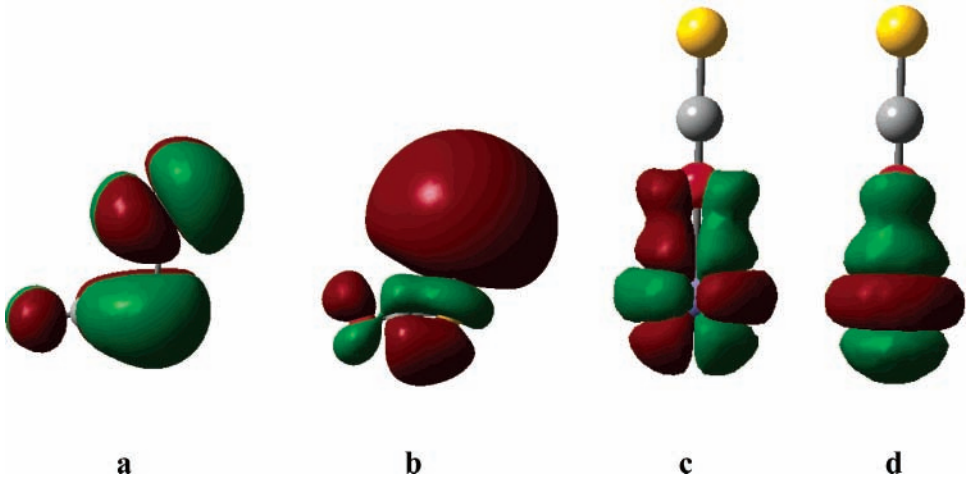

Figure 5. Orbital interaction iso-surfaces of the initial complexes for (a) the HOMO of ^{4}**1**, (b) the LUMO of ^{4}**1**, (c) the HOMO of ^{4}**3**, and (d) the LUMO of ^{4}**3**.

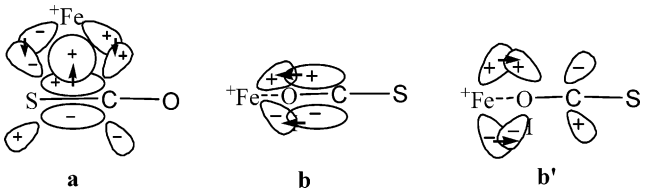

Figure 6. Sketch of the orbital interactions between Fe^+ and OCS for (a) the initial sulfur-bound complex and for (b) and (b′) the initial oxygen-bound complex.

may return to the sextet surface during the conversion of $\mathbf{TS_{3-4}}$ to intermediate **4**.

3.6. Comparison between the C−S and C−O Bond Activations. On the basis of our calculations, it is clear that the C−S bond activation is much easier than the C−O bond activation. This is not difficult to understand in view of the lower C−S bond energy compared to that of the C−O bond. To achieve a deeper comprehension of the C−S and C−O bond activations, we further analyze here the relevant intrinsic properties. As shown in Figure 2, we noted that the sulfur-bound encounter complexes, ^{4}**1** and ^{6}**1**, have bent geometries, whereas the oxygen-bound ones, ^{4}**3** and ^{6}**3**, are linear and almost linear, respectively. This fact suggests that the orbital interaction between Fe^+ and OCS is not same in the two initial complexes. As an example, Figure 5 shows the HOMO and LUMO isosurfaces of ^{4}**1** and ^{4}**3**. Clearly, in both complexes, the HOMOs mainly consist of the π orbital of the C−O or C−S bond and a 3d orbital of Fe^+ (see Figure 5a,c). However, the composition of LUMO differs in two complexes. As shown Figsure 5b,d, the LUMO of the sulfur-bound complex (^{4}**1**) mainly comes from the 4s orbital of Fe^+ and the π^* orbital of C−S bond, whereas for the oxygen-bound complex, the LUMO is determined by a 3d orbital of Fe^+ and the π^* orbital of C−O bond. From these isosurfaces, the picture of orbital interactions between Fe^+ and OCS in ^{4}**1** and ^{4}**3** is now clear, as schematically shown in Figure 6. For the sulfur-bound structure (^{4}**1**), the π electrons of C−S bond transfer into the empty 4s orbital of Fe^+ (Figure 6a), whereas for the oxygen-bound complex (^{6}**1**), the π electrons of C−O bond transfer into an energetically higher 3d orbital of Fe^+ (Figure 6b), which is less favorable than transferring into the 4s orbital of Fe^+. In both structures, the d electrons of Fe^+ donate back into the π^* orbital of the C−S or C−O bond (Figure 6a,b′) to enhance the interaction between Fe^+ and COS. These orbital analyses clearly indicate that the bent structure provides a relatively better position to insert Fe^+ into the C−S bond, thereby explaining why the C−S bond activation is easier than the C−O bond activation using Fe^+ as the catalyst.

3.7. Reaction of Fe^+ with OCS vs Its Reaction with CS_2. In a recent paper,[9] we reported the reaction of Fe^+ with CS_2, where the C−S bond activation was characterized by a high barrier of 38.9 kcal mol^{-1} for Fe^+ inserting into a C−S bond. All the experimentally observed products from the reaction of Fe^+ with CS_2 had been rationalized according to the insertion−elimination mechanism. From the present study, we found this mechanism also applies to the reaction of Fe^+ with OCS; however, the barrier for the C−S bond activation is only 15.8 kcal mol^{-1}, much less than that of $Fe^+ + CS_2$. This behavior is in line with an earlier experiment by Rue,[8] where the threshold of the FeS^+ cross section was shifted to lower energy in the reaction of Fe^+ with OCS. Obviously, this is because the C−S bond energy in OCS is much lower than in CS_2. Although the direct sulfur atom abstractions by Fe^+ could also contribute to the formations of FeS^+ in both reactions, our calculations do not provide evidence for this direct abstract mechanism. In addition, this insertion−elimination mechanism is also observed in the reaction of V^+, an early first-row transition metal ion, with the CS_2 system.[36] From these facts, we conjecture that the insertion−elimination reaction could be a general mechanism for the reactions of first-row transition ions with small sulfide molecules.

Further, the global minimum on the PES of $[Fe, C, S_2]^+$ is a carbon-bound complex between Fe^+ and CS_2,[9] whereas this structure is not found for $Fe^+ +$ OCS system. Instead, the present calculations identified a sulfur-bound initial complex as the global minimum on the PES of $[Fe, C, O, S]^+$. By comparing geometries of these global minima, we found the Fe−S distance (2.386 Å) in the sulfur-bound complex is much longer than the corresponding Fe−C distance (1.950 Å) in the carbon-bound complex.[9] This behavior indicates that the interaction between Fe^+ and OCS is different in nature from that between Fe^+ and CS_2: the bonding in the sulfur-bound complex is primarily electrostatic in character, whereas the bonding in the carbon-bound complex involves covalent property. This difference in bonding property can rationalize the fact the C−S bond activation in OCS is energetically more favorable than that in CS_2.

4. Conclusion

The reaction of Fe^+ toward OCS proceeds according to the insertion−elimination mechanism, which can rationalize all

observed products in early experiments. The direct sulfur and oxygen atom abstractions by Fe^+ could also be possible to contribute to the formations of FeS^+ and FeO^+; however, the tight transition state structures cannot be formed in these reactions. The intersystem crossing behavior between the quartet and sextet surfaces of $[Fe, C, O, S]^+$ would occur easily because the splitting of the two surfaces is small. The C−S bond activation is energetically much more favorable than the C−O bond activation. The energetically most favorable reaction channel is $Fe^+(^6D) + OCS \rightarrow FeS^+(^6\Sigma_g) + CO$, which is endothermic by 1.8 kcal mol^{-1}, whereas the reaction $Fe^+(^6D) + OCS \rightarrow FeO^+(^6\Sigma_g) + SO$ is only feasible at elevated energies, and endothermic by 79.3 kcal mol^{-1}.

Acknowledgment. This work was supported by the Natural Science Foundations of China (No. 20073024 and No. 20133020) and the Natural Science Foundation of Shandong province (No. Y2002B02).

References and Notes

(1) Stiefel, E. I. In *Transition Metal Sulfur Chemistry*; Stiefel, E. I., Matsumoto, K., Eds.; ACS Symposium Series 653; American Chemical Society: Washington, DC, 1996.
(2) Stiefel, E. I. In *Kirk-Othmer Encyclopedia of Chemical Technology*, 4th ed.; 1995; Vol. 16, pp 940−962.
(3) Bryant, R. D.; Kloeke, F. V. O.; Laishley, E. J. *Appl. Environ. Microbiol.* **1993**, *59*, 491.
(4) Farr, J. P. G. *Wear* **1975**, *35*, 1.
(5) Miki, Y.; Nakazato, D.; Ikuta, H.; Uchida, T.; Wakihara, M. *J. Power Sources* **1995**, *54*, 508.
(6) Holm, R. H. *Chem. Rev.* **1996**, *96*, 2237.
(7) Kaim, W.; Schwederski, B. *Bioinorganic Chemistry*: *Inorganic Elements in the Chemistry of Life*; J. Wiley & Sons: New York, 1994.
(8) Rue, C.; Armentrout, P. B.; Kretzschmar, I.; Schroder, D.; Schwarz, H. *J. Phys. Chem. A* **2001**, *105*, 8456.
(9) Jiang, N.; Zhang, D. J. *Chem. Phys. Lett.* **2002**, *366*, 253.
(10) Pedley, J. B.; Naylor, R. D.; Kirby, S. P. *Thermochemical Data of Organic Compounds*; Chapman and Hall: London, 1986.
(11) Prinslow, D. A.; Armentrout, P. B. *J. Chem. Phys.* **1991**, *94*, 3563.
(12) Parr, R. G.; Yang, W. *Density Functional Theory of Atom and Molecules*; Oxford University Press: New York, 1989.
(13) Kryachko, E. S.; Ludena, E. V. *Electron Densith Functional Theory of Many-Electron Systems*; Kluwer: Dordrecht, The Netherlands, 1990.
(14) Becke, A. D. *J. Chem. Phys.* **1993**, *98*, 1372.
(15) Lee, C.; Yang, W.; Parr, R. G. *Phys. Rev. B* **1988**, 37, 785.
(16) Davidson, E. R. *Chem. Rev.* **2000**, *100*, 351.
(17) Pavlov, M.; Siegbahn, P. E. M.; Sandstrom, M. *J. Phys. Chem. A* **1998**, *102*, 219.
(18) Aschi, M.; Bronstrup, M.; Diefenbach, M.; Harvey, J. N.; Schroder, D.; Schwarz, H. *Angew. Chem., Int. Ed.* **1998**, *37*, 829.
(19) Yi, S. S.; Blomberg, M. R. A.; Siegbahn, P. E. M.; Weisshaar, J. C. *J. Phys. Chem. B* **1998**, *102*, 395.
(20) Zhang, D. J.; Liu, C. B.; Bi, S. W.; Yuan, S. L. *Eur. Chem. J.* **2003**, *9*, 484.
(21) Hoch, W.; Holthausen, M. C. *A Chemist's Guide to Density Functional Theory*; Wiley-VCH: Weinheim, 2000.
(22) McLean, A. D.; Chandler, G. S. *J. Chem. Phys.* **1980**, *72*, 5639.
(23) Hay, P. J. *J. Chem. Phys.* **1977**, *66*, 4377.
(24) Barsch, S.; Schroder, D.; Schwarz, H. *J. Phys. Chem. A*, **2001**, *105*, 2005.
(25) Gonzalez, C.; Schlegel, H. B. *J. Phys. Chem.* **1990**, *94*, 5523.
(26) Frisch, M. J.; Trucks, G. W.; Schlegel, H. B.; Scuseria, G. E.; Robb, M. A.; Cheeseman, J. R.; Zakrzewski, V. G.; Montgomery, J. A., Jr.; Stratmann, R. E.; Burant, J. C.; Dapprich, S.; Millam, J. M.; Daniels, A. D.; Kudin, K. N.; Strain, M. C.; Farkas, O.; Tomasi, J.; Barone, V.; Cossi, M.; Cammi, R.; Mennucci, B.; Pomelli, C.; Adamo, C.; Clifford, S.; Ochterski, J.; Petersson, G. A.; Ayala, P. Y.; Cui, Q.; Morokuma, K.; Malick, D. K.; Rabuck, A. D.; Raghavachari, K.; Foresman, J. B.; Cioslowski, J.; Ortiz, J. V.; Stefanov, B. B.; Liu, G.; Liashenko, A.; Piskorz, P.; Komaromi, I.; Gomperts, R.; Martin, R. L.; Fox, D. J.; Keith, T.; Al-Laham, M. A.; Peng, C. Y.; Nanayakkara, A.; Gonzalez, C.; Challacombe, M.; Gill, P. M. W.; Johnson, B. G.; Chen, W.; Wong, M. W.; Andres, J. L.; Head-Gordon, M.; Replogle, E. S.; Pople, J. A. *Gaussian 98*, revision A.9; Gaussian, Inc.: Pittsburgh, PA, 1998.
(27) *NIST-JANAF Thermochemical Tables*, 4th ed.; Chase, M. W., Ed.; I. *Phys. Chem. Ref. Data*, Monograph No. 9. American Chemical Society: Washington, DC, 1998.
(28) Armentrout, P. B.; Kickel, B. L. In *Organometallic Ion Chemistry*; Freiser, B. S., Ed.; Kluwer Academic: Dordrecht, 1996; p28.
(29) Schroder, D.; Kretzschmar, I.; Schwarz, H.; Rue, C.; Armentrout, P. B. *Inorg. Chem.* **1999**, *38*, 3474.
(30) Schultz, R. H.; Crellin, K.; Armentrout, P. B. *J. Am. Chem. Soc.* **1991**, *113*, 8590.
(31) Lahaye, J. G.; Vandenhaute, R.; Fayt, A. *J. Mol. Spectrosc.* **1987**, *123*, 48.
(32) Sugar, J.; Corliss, C. *J. Phys. Chem. Ref. Data. Suppl.* **1985**, *14*, 1.
(33) Ziegler, T.; Li, J. *Can. J. Chem.* **1994**, *72*, 783.
(34) Harvey, J. N.; Heinemann, C.; Fiedler, A.; Schroder, D. *Chem. Eur. J.* **1996**, *2*, 1230.
(35) Yumura, T.; Amenomori, T.; Kagawa, Y.; Yoshizawa, K. *J. Phys. Chem. A* **2002**, *106*, 621.
(36) Rue, C.; Armentrout, P. A. *J. Chem. Phys. A* **1999**, *110*, 7858.